Enhanced Motor Imagery Based Brain-Computer Interface via FES and VR for Lower Limbs

Shixin Ren, Weiqun Wang, *Member, IEEE*, Zeng-Guang Hou, *Fellow, IEEE*, Xu Liang, Jiaxing Wang, *Graduate Student Member, IEEE*, and Weiguo Shi

***Abstract*— Motor imagery based brain-computer interface (MI-BCI) has been studied for improvement of patients' motor function in neurorehabilitation and motor assistance. However, the difficulties in performing imagery tasks limit its application. To overcome the limitation, an enhanced MI-BCI based on functional electrical stimulation (FES) and virtual reality (VR) is proposed in this study. On one hand, the FES is used to stimulate the subjects' lower limbs before their imagination to make them experience the muscles' contraction and improve their attention on the lower limbs, by which it is supposed that the subjects' motor imagery (MI) abilities can be enhanced. On the other hand, a ball-kicking movement scenario from the first-person perspective is designed to provide visual guidance for performing MI tasks. The combination of FES and VR can be used to reduce the difficulties in performing MI tasks and improve classification accuracy. Finally, the comparison experiments were conducted on twelve healthy subjects to validate the performance of the enhanced MI-BCI. The results show that the classification performance can be improved significantly by using the proposed MI-BCI in terms of the classification accuracy (ACC), the area under the curve (AUC) and the F1 score (paired t-test, p <0.05).**

***Index Terms*— Brain computer interface, functional electrical stimulation (FES), virtual reality, enhanced motor imagery, rehabilitation training.**

Manuscript received November 8, 2019; revised March 30, 2020 and May 3, 2020; accepted June 6, 2020. Date of publication June 12, 2020; date of current version August 7, 2020. This work was supported in part by the National Natural Science Foundation of China under Grant 91648208, Grant 91848110, and Grant 61720106012 and in part by the Beijing Natural Science Foundation under Grant 3171001 and Grant 4202074. *(Corresponding author: Weiqun Wang.)*

Shixin Ren, Xu Liang, Jiaxing Wang, and Weiguo Shi are with the State Key Laboratory of Management and Control for Complex Systems, Institute of Automation, Chinese Academy of Sciences, Beijing 100190, China, and also with the School of Artificial Intelligence, University of Chinese Academy of Sciences, Beijing 100490, China (e-mail: renshixin2015@ia.ac.cn; liangxu2013@ia.ac.cn; wangjiaxing2016@ia.ac.cn; shiweiguo2017@ia.ac.cn).

Weiqun Wang is with the State Key Laboratory of Management and Control for Complex Systems, Institute of Automation, Chinese Academy of Sciences, Beijing 100190, China (e-mail: weiqun.wang@ia.ac.cn).

Zeng-Guang Hou is with the State Key Laboratory of Management and Control for Complex Systems, Institute of Automation, Chinese Academy of Sciences, Beijing 100190, China, also with the University of Chinese Academy of Sciences, Beijing 100049, China, and also with the CAS Center for Excellence in Brain Science and Intelligence Technology, Beijing 100190, China (e-mail: zengguang.hou@ia.ac.cn).

Digital Object Identifier 10.1109/TNSRE.2020.3001990

I. Introduction

BRAIN-COMPUTER interfaces (BCIs) can be used to provide communication pathways between human brains and the external devices, and have been widely studied in neurorehabilitation and motor assistance [1]–[3]. Motor imagery (MI) is a typical brain activity, which is often used in BCI and can be defined as the mental rehearsal of limb movements without actual execution [4], [5]. The motor cortex region activated by MI is similar to that activated by actual execution. Motor imagery based brain-computer interface (MI-BCI) has been designed for reconstructing the damaged neuro-pathways [6], [7] and improving patients' motor function [8]–[10]. However, there are significant individual differences in the MI capability for different subjects, and it is very difficult to perform MI tasks for some subjects. Meanwhile, due to that EEG signals arose from brain activities during performing MI are relatively weak and easily affected by noises, it is difficult to obtain the high recognition accuracy. These difficulties limit the applications of MI-BCI.

Many methods have been proposed for improvement of the classification accuracy [11], [12]. For instance, denoising and feature extraction algorithms have been applied to enhance the signal to noise ratio and improve the discriminability of MI patterns [13], [14]. Since the recorded electroencephalography (EEG) data usually consists of multi-channel signals, the channel selection methods have been studied for selecting the key channels that have significant contributions to improvement of recognition accuracy [15], [16]. Recently, the generalization capability of EEG classification models was improved by using deep learning (DL) methods, where signal preprocessing, feature extraction, and classification were integrated in one model [17], [18]. Especially for the large-scale MI database, DL methods have shown the superior performance and promising potential in improvement of the classification accuracy than conventional approaches [19]. From the results mentioned above, these state-of-the-art methods are indeed helpful for overcoming the difficulties in MI pattern recognition tasks. However, it is still difficult to obtain high recognition accuracy since subjects usually cannot perform MI tasks well [20], and the EEG signal quality of MI has a critical effect on the recognition accuracy. Therefore, many attentions

have been paid to help subjects perform MI effectively and improve subjects' MI capability for obtaining the high quality EEG signals.

In traditional MI experiment paradigms, arrows or texts are often used as the cues for the imagery tasks. For example, subjects imagined the left or right-hand movement according to the arrow direction [21]. However, the cues given by arrows or texts were usually very abstract, so that it is difficult for subjects to imagine the movements. According the subjects' feedback in [22], using the traditional experiment paradigm made them feel tired and distracted easily.

The vivid visualization scenarios have been suggested to replace the arrow or text cues to instruct subjects for performing MI relatively effectively [23], [24]. Bian *et al.* [25] found that dynamic video guidance was more helpful than static photo guidance for improvement of classification performance. From [26], it can be seen that the discriminability of imagined patterns could be enhanced significantly by using the object-directed scenario as the guidance, and the average recognition accuracy based on the object-directed scenario was 7% higher than that based on the non-object-directed scenario. Sollfrank *et al.* [24] investigated the advantages of the 3D limb movement guidance over the 2D limb movement guidance. From the comparison experiment results, it can be found that the 3D movement guidance was more effective than the 2D movement guidance in enhancing motor cortex activation. Qiu *et al.* [22] designed a novel MI paradigm for guiding subjects to modulate brain activity effectively, where subjects were required to imagine writing Chinese characters according to the picture cue. As shown in the experiment results of [22], higher motor cortex activation and classification accuracy could be obtained by imaging writing Chinese characters, as opposed to the traditional paradigm (i.e., the arrows). However, for some subjects, the vivid visual guidance may make them concentrate on the moving objects instead of performing MI tasks.

To help subjects modulate brain activity effectively, various kinds of feedback have been adopted in the MI-BCI systems. In [27], Dariusz *et al.* investigated the impact of different types of feedback provided in training on the MI-BCI's performance. Bhattacharyya *et al.* [28] found that the functional electrical stimulation (FES) based feedback was more effective than the visual feedback for cortical learning and improving classification accuracy. In [29], the kinesthetic feedback provided by a robotic orthosis and visual feedback were used and compared in the online control. As shown in the comparison results, the online classification accuracy were improved significantly by the kinesthetic feedback. However, it has been proven that the feedback can have inhibitory as well as facilitory effects on EEG control [30]. The performance of feedback could be affected by the initial classifier, which is generally modeled based on calibration data without feedback [22]. For the subjects who are unfamiliar with MI, the excessive unintended or inaccurate feedback/control may frustrate them [31]. The suitable imagination guidance paradigms would help subjects reduce frustration. In addition, the enhanced MI-BCI have been studied mostly on the upper limb MI. While the number of studies on the lower limb MI is relatively small [32], [33], due to the particular difficulties in implement of motor imagery for lower limbs.

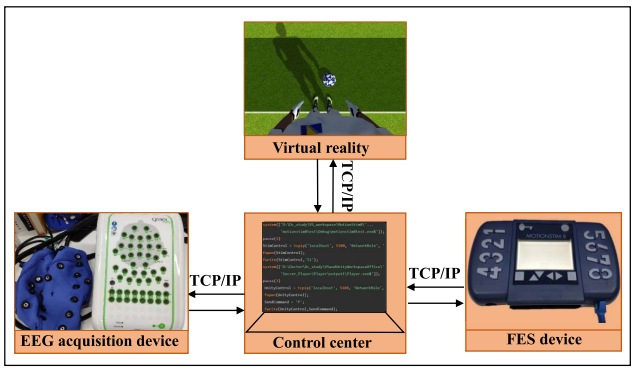

Fig. 1. The enhanced MI-BCI system. The FES device and virtual reality scenario are controlled by commands from the control center. TCP/IP protocol is used for data and command transmission.

In this study, an enhanced MI-BCI based on FES and virtual reality (VR) scenario is proposed to improve subjects' MI abilities and the recognition accuracy. The VR scenario is designed to provide the visual guidance, where the advantages of dynamic video guidance [25] and object-directed scenario [26] are combined effectively. In addition to the visual guidance, FES technology is adopted as an additional enhancement mode to improve subjects' attention on the associated lower limb. By the comparison experiments carried out in this study, it is verified that the classification accuracy and the subjects' motor cortex activation can be improved by using the proposed MI-BCI.

The remainder of this paper is organized as follows. The design of the enhanced MI-BCI system is introduced in Section II. The EEG data processing, the feature extraction method, the classification algorithm, and data analysis methods are described in Section III. Section IV presents the comparison experiments and the results. Finally, the discussion and conclusion are given in Section V and VI, respectively.

II. Design of the Enhanced MI-BCI

An enhanced MI-BCI based on FES and VR is designed in this study, where the FES device (MotionStim8), the EEG acquisition system (NeuroScan system including Quick-cap, Grael amplifier, and Curry8 software), the virtual reality scenario based on Unity3D, and the control center (one computer installed MATLAB) are used, as shown in Fig. 1. Firstly, according to the commands from the control center, the right lower limb's muscles are stimulated by the FES produced from MotionStim8. Then, the virtual reality scenario is showed on the screen for providing the guidance to subjects during performing MI. Meanwhile, the brain activity is recorded by NeuroScan system and transferred to the control center for data processing and analysis. The data transmission between each part and the control center is achieved via TCP/IP, by which the reliability and low delay of communication can be guaranteed.

A. EEG Signal Recording

EEG signals were recorded at the sampling rate of 256Hz by the NeuroScan system. There are 32 channels on the

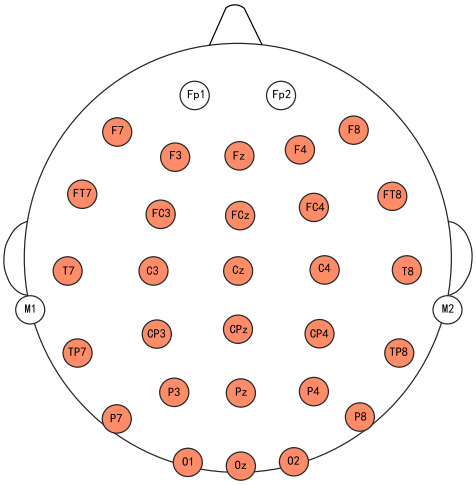

Fig. 2. The channel (or electrode) distribution of the Quick-cap. EEG signals from the salmon channels were used for recognition and the subsequent analysis, and the signals from the white channels were not considered in this study.

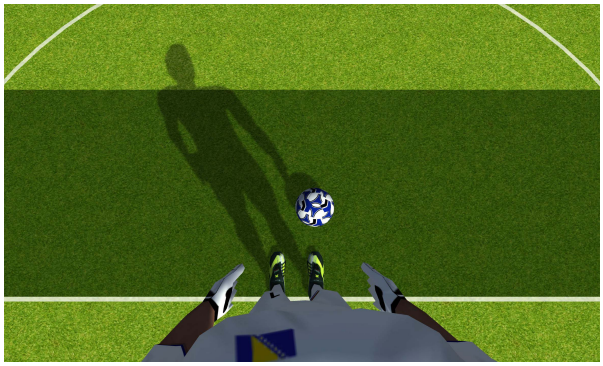

Fig. 3. The designed ball-kicking scenario based on unity3D. The right lower limb of avatar can be controlled by the external commands to kick the ball.

Quick-cap, and the channels are placed according to the International 10/20 System. The signals from channels M1 and M2 have little relationship with the MI brain activities and are usually used as the reference signals. Meanwhile, since the signals from channels Fp1 and Fp2 are affected significantly by the eye-blink and have little relationship with the MI brain activities as well. Therefore, the signals from these four channels were not considered in this study, and the signals from 28 channels (i.e., the salmon channels in Fig. 2) were further processed and analyzed. Additionally, the common average reference has been used as the reference method in this study, which was recommended by [34] for MI analysis and can be used to improve the signal-to-noise ratio. It has been proven that the EEG signals in the low-frequency band (8-32Hz) have a high correlation with the brain activity of MI [35], and the EEG signals below 50Hz are usually used for the classification and analysis [36], [37]. Thus the raw EEG signals were filtered by bandpass filter (0.1-50Hz) in this study, which was implemented in Curry 8.

The channels on Quick-cap are connected to the scalp through the conductive gel. To guarantee the quality of the collected EEG signals, the impedance between the channels and the scalp should be stable and as low as possible. Hence, after the channels were injected with the conductive gel, subjects were required to wait a few minutes to make the impedance table and drop below 10 $K\Omega$.

B. The Design of Virtual Reality Scenario

To provide an effective visual guidance, a ball-kicking movement (BKM) scenario is designed based on the Unity3D development software, as shown in Fig. 3. The first-person perspective is adopted in the scenario to provide an immersive environment to subjects. The lasting time of the BKM scenario is four seconds, which is composed of three seconds for the action and one second for the static posture. In addition, an interaction pathway is established via TCP/IP between the scenario and the external devices, and the avatar in the scenario can be controlled by the external commands.

C. The Design of FES-Enhancement

FES technology has been widely applied in motor rehabilitation for restoring patients' motor function [38], [39]. The muscle contraction caused by FES can make subjects produce the kinesthesia illusion, which is an effective guidance for subjects to perform MI. Moreover, the muscle contraction feeling is helpful to improve the subjects' attention on the associated limbs. Based on the above reasons, it is supposed that the subjects' MI effects can be improved by using the FES as the guidance.

In this study, MotionStim8 (MEDEL company, Germany) device was used to provide the current stimulation, which is a biphasic rectangular pulse shape and can effectively prevent muscle fatigue. The current, pulse width and interval times can be programmatically adjusted. In the actual ball-kicking movement, the relatively obvious contraction can be found in the tibialis anterior muscle (TA) and rectus femoris muscle (RF). Therefore, the TA and RF muscles of right lower limb are selected to give the FES, by which the subjects can experience the similar muscle contraction sensation produced by the actual BKM. The muscle contraction strength is depend on FES's current amplitude, and the high current value can induce the limb's actual movement [40]. However, the discomfort caused by the high current value may lead to the reduction of subjects' active participation. Hence, FES's current amplitude should be set to an appropriate value, which can only induce slight muscle contraction and cannot induce the limb movement.

The pre-experiments were conducted to decide the current amplitude according to the subjects' feedback. In this study, th stimulation current amplitudes of TA and RF muscles were set to 24∼26 mA and 10∼12 mA, respectively; moreover, the pulse width and stimulation frequency were set to 100μs and 30Hz, respectively. The stimulation time was set to 3s to be in harmony with the BKM scenario. The stimulation period and the current change process are shown in Fig. 4.

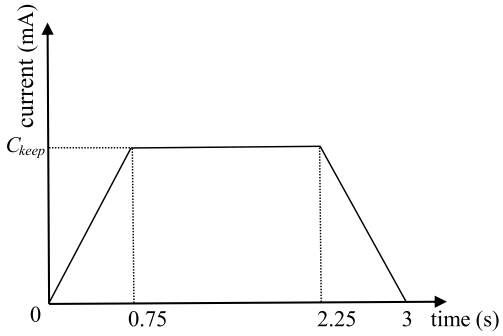

Fig. 4. The current curve of FES. Three line-segments are respectively corresponding to three phases of the BKM scenario, i.e., start, keep and relax. The stimulation current amplitudes, C_{keep}, for TA and RF muscles are 24 ∼ 26 mA and 10 ∼ 12 mA, respectively.

III. Data Processing, Feature Extraction, Classification and Analysis Methods

A. EEG Signal Processing

In this paper, each MI task lasts four seconds (i.e., 1024 sampling points) in one trial. In order to obtain more training samples and improve classification performance, the sliding-window method is adopted to process EEG signals. At the beginning of EEG signals, a window with the length of 512 sampling points was placed and slid along the time axis at intervals of 256 sampling points. Hence, four-second EEG signals were divided into three segments, and every segment contains 28×512 sampling points.

Then, EEG signals in every window are regarded as a sample, which is used to extract the features for classification. Due to that there is some overlap among the three windows from one trial, the correlation between them is relatively high. Therefore, to evaluate the classification performance accurately, it should be noted that when dividing the training and testing set, the division of samples should be based on the trial rather than the sample, i.e., the three samples from the one trial can only put into training or testing set at the same time.

B. Feature Extraction and Classification Algorithm

The common spatial pattern (CSP) algorithm [41] has been adopted widely in EEG signal feature extraction for its good performance [42], [43]. It has been proven that the EEG signal frequency is a key factor affecting the performance of CSP [44]. Therefore, EEG signals can be divided into sub-frequency band signals by adopting multiple bandpass filters and then using CSP to extract the features of each sub-frequency band signals. As shown in the results of [37], [45], [46], the classification accuracy could be improved significantly by extracting features from the sub-frequency band signals. Hence, the sub-frequency band division and CSP methods are combined to extract the EEG features in this paper.

Let S^k denotes an EEG signal sample, where $k = 1, 2$ represents the imagined pattern. The dimensions of S^k are $M \times N$, where M and N are the numbers of channels and sampling points, respectively. Firstly, S^k are filtered into ten sub-frequency bands at the intervals of 4Hz (i.e., [1-4Hz], [5-8Hz], …, [37-40Hz]). The i-th sub-frequency band signal is represented by $S_i^k \in \mathbb{R}^{M\times N}$ $(i = 1, \ldots, 10)$. Then the normalized covariance matrix of S_i^k can be calculated by:

$$C_i^k = \frac{S_i^k (S_i^k)^T}{\text{trace}(S_i^k (S_i^k)^T)}, \tag{1}$$

where T denotes the transpose. For the multiple samples, the matrices $\overline{C_i^k}$ denotes the mean of all sample covariance matrices.

The goal of CSP is to find a transformation matrix $W_i \in \mathbb{R}^{M\times M}$, by which the discrimination between two patterns can be maximized. The transformation matrix W_i can be calculated by maximizing the following equation:

$$J(W_i) = \frac{W_i^T \overline{C_i^1} W_i}{W_i^T \overline{C_i^2} W_i}. \tag{2}$$

More details of solving Eq. (2) was given in [41]. After the transformation matrix W_i is obtained, the EEG signals S_i^k can be transformed by:

$$Z_i^k = W_i S_i^k. \tag{3}$$

The most discrimination information between S_i^1 and S_i^2 can be obtained from the variances of the transformed signals Z_1^k and Z_2^k. Generally, the first m and last m $(m < \frac{M}{2})$ rows of the transformed signals Z_i^k, i.e. $Z_{i,r}^k$ $(r = 1, \ldots, 2m)$ are used to extract features, as follows:

$$f_{i,r}^k = log\left(\frac{\text{var}(Z_{i,r}^k)}{\sum_{j=1}^{2m} \text{var}(Z_{i,j}^k)}\right), \tag{4}$$

In this paper, $m = 2$ is adopted for high classification accuracy and low calculation load. Therefore, for each transformed sub-frequency band signals Z_i^k, 4 features $([f_{1,1}^k, \ldots, f_{1,4}^k])$ can be calculated by Eq. (4) to form a vector f_i^k. Due to that S^k are filtered into ten sub-frequency bands, the features of ten sub-frequency bands are integrated into $F^k = [f_1^k, \ldots, f_{10}^k]$ $(F^k \in \mathbb{R}^{1\times 40})$ as the feature vector of S^k. Finally, all feature vectors F were used to train the classifier. The flow chart of the feature extraction and classification is given in Fig. 5.

Support vector machine (SVM) has great advantages in the classification of small samples and binary classification problem [47]. Since the number of samples in this study is relatively small, SVM has been adopted as the classifier. Libsvm tool [48] of MATLAB platform was used to construct the SVM model and the radial basis function (RBF) was used as the kernel function. Meanwhile, parameter "C" in the cost function and parameter "γ" in the RBF are determined by the grid optimization method.

C. Data Analysis Methods

In this study, there are two MI tasks: imaginations of the BKM and the idle states. The BKM state is regarded as the positive label, and the idle state is regarded as the negative label. To compare the performance of classification models, several metrics are adopted: accuracy (ACC), F1 score, and area under receiver operating characteristic curve (AUC).

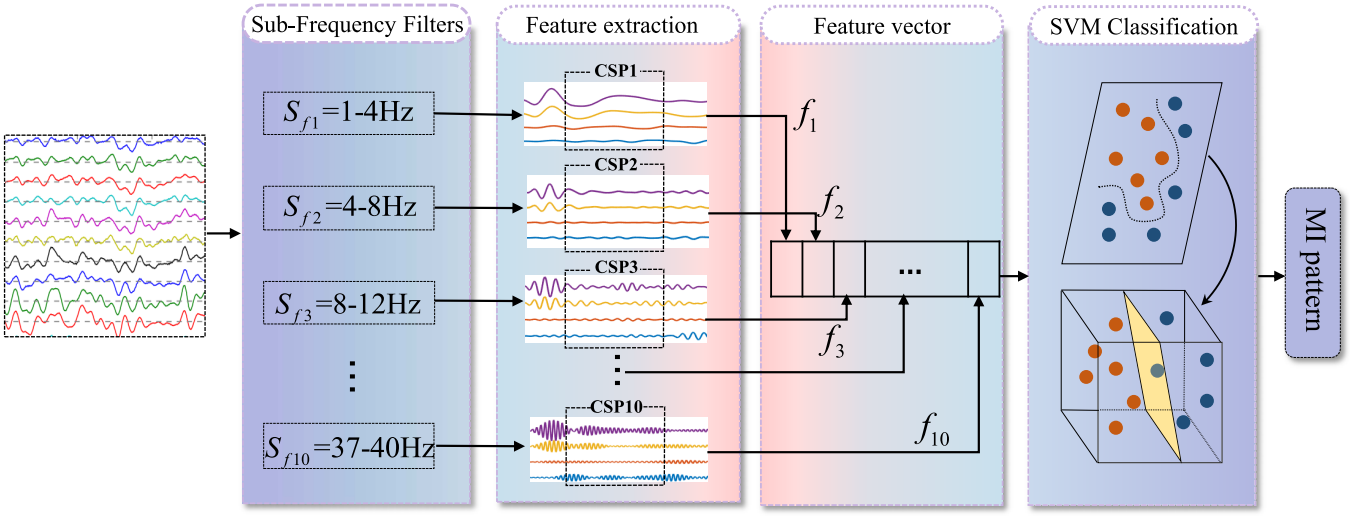

Fig. 5. The flow chart of MI pattern classification using sub-frequency band information, CSP and SVM. The pre-processed EEG signals are filtered into ten sub-frequency band signals by ten band-pass filters. Each feature vector f_i (i=1,…,10) is extracted from the associated sub-frequency band signals using CSP. Ten feature vectors are combined to form a single vector as the input of the SVM classifier.

The calculations of ACC and F1 score are as follows:

$$\text{ACC} = \frac{\text{TP} + \text{FN}}{\text{TP} + \text{FP} + \text{TN} + \text{FN}}, \tag{5}$$

$$\text{F1 score} = 2 \cdot \frac{\text{TP}/(\text{TP} + \text{FP}) \cdot \text{TP}/(\text{TP} + \text{FN})}{\text{TP}/(\text{TP} + \text{FP}) + \text{TP}/(\text{TP} + \text{FN})}, \tag{6}$$

where TP, FP, TN, and FN are the sample numbers of true positives, false positives, true negatives, and false negatives, respectively. In this study, ten fold cross-validation was adopted and repeated ten times; then, the average of all accuracy values was used as the final accuracy.

The activation of the motor cortex induced by MI can result in the reduction of EEG signal power [35], [49]. The power spectral density (PSD) method is usually applied to analyze the changes of EEG signal power and further evaluate the activation intensity of the motor cortex.

The signals of channels C3, Cz, and C4 are from the motor cortex region, and they have a relatively high correlation with the limb movement imagery. Hence, these signals are usually used for the activation intensity analysis in the statistic. The changes of activation intensity are significant in the 8-30Hz frequency region, which mainly includes α (8-13Hz) and β (14-30Hz) rhythms. To obtain the detailed analysis, the PSD changes of EEG signals in α, β, and $\alpha + \beta$ rhythms are calculated for the comparison.

The distribution normality of the experimental metrics (i.e., ACC, AUC, F1 score, and PSD values) was validated using the lilliefors test algorithm of MATLAB (2016b). Then, one-way analysis of variance (one-way ANOVA) and the paired t-test method were adopted to analyze the significant difference between the experiment results for the VR and FES+VR paradigms.

IV. Experiment and Results

A. Experimental Design

In order to validate the performance of the proposed MI-BCI, two experiment paradigms were designed according to whether there is FES-enhancement, as shown in Fig. 6. The experiment process is described in more detail below.

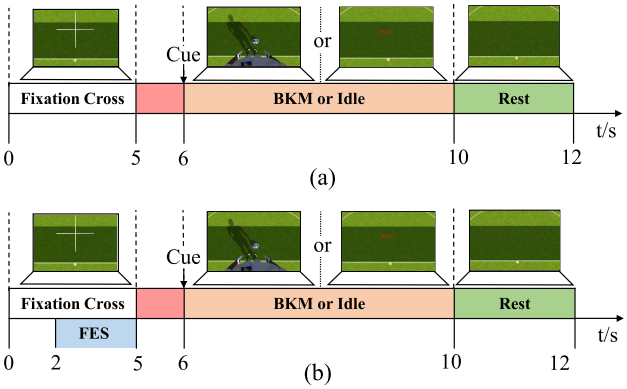

Fig. 6. (a) VR, and (b) FES+VR experiment paradigms. In each trial, the fixation cross was used to remind subjects to stay focused. Subjects were required to perform the BKM or Idle imagery task according to the cue; meanwhile, a corresponding virtual reality scenario was shown on the screen to provide the visual guidance. In the FES+VR paradigm, FES was given to subjects from 2s to 5s.

Due to the difference of each subject's physical situation, the maximum FES current amplitude was slightly adjusted within 3 mA according to the subject's feedback. Then subjects were instructed to sit in a comfortable chair about 70 cm away from the display screen. All subjects were informed and familiar with the procedures before the experiment. During the experiment, subjects were required to avoid the movements and keep quiet.

Each experiment paradigm consists of two tasks: imaginations of the BKM and the idle states. As shown in Fig. 6, each trial lasts about 12s. At the beginning (t = 0s) of each trial, a fixation cross was displayed on the screen to remind subjects to stay focused. In the experiment paradigm with FES-enhancement (i.e., FES+VR), subjects were given three-second FES at t = 2s, and not required to perform

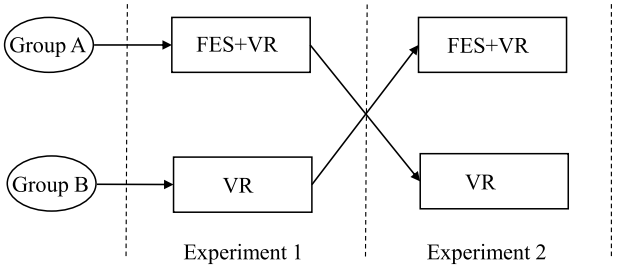

Fig. 7. The experimental scheme. For subjects of group A, the FES+VR and VR paradigms were used in experiment 1 and 2, respectively. For subjects of group B, the VR and FES+VR paradigms were used in experiment 1 and 2, respectively.

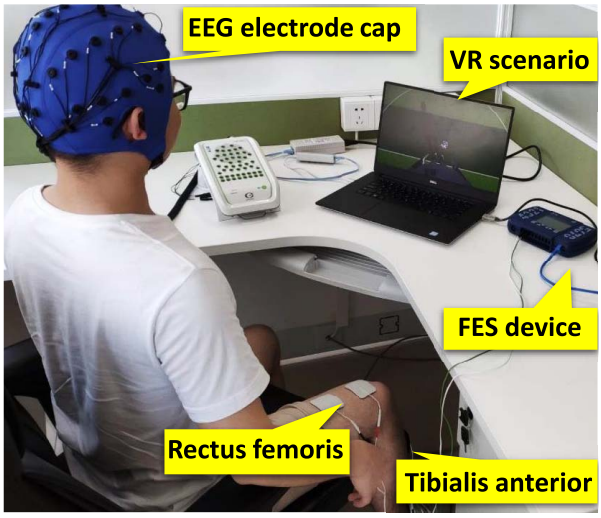

Fig. 8. A subject was performing BKM task based on the FES+VR paradigm. Subject's TA and RF muscles were attached with the FES electrodes; and EEG signals were recorded using the NeuroScan system and transmitted to the control center (PC) for data processing.

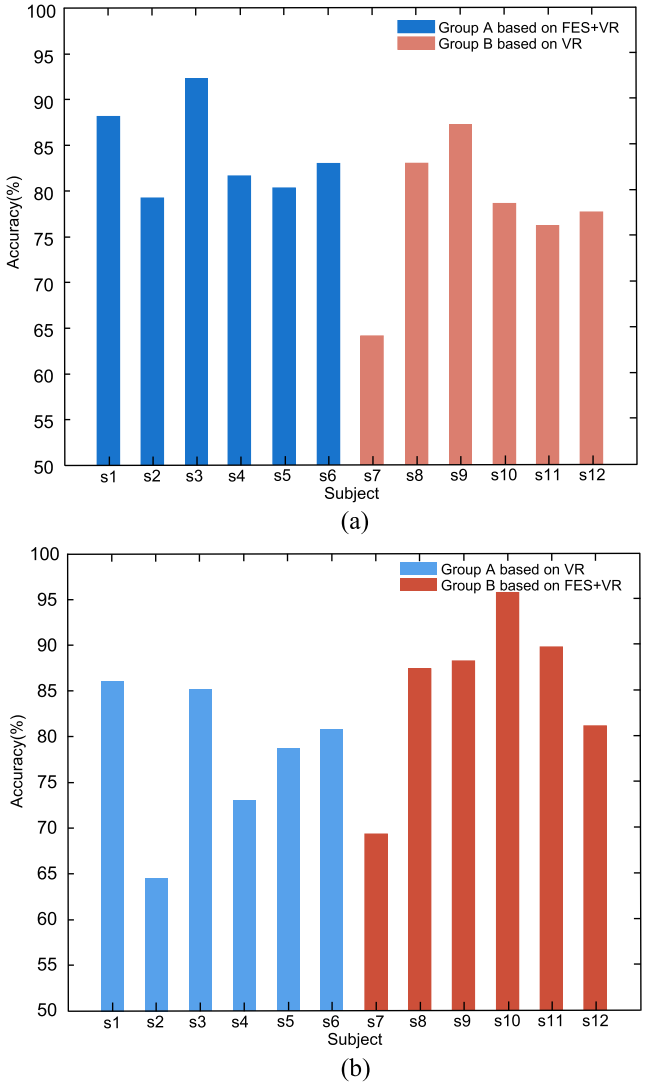

Fig. 9. The classification accuracies for 12 subjects in (a) experiment 1, and (b) experiment 2.

any tasks during this time. After that, there is a one-second interval to reduce the possible delayed impacts from FES. Then the task text cue was displayed at t = 6s, and subjects were required to imagine the corresponding state for four seconds according to the cue. When subjects imagined BKM, the designed BKM animation was shown to subjects synchronously. When subjects imagined the idle state, the avatar was removed and there was only the background on the screen. After the imagination (t = 10s), the rest cue was displayed to remind subjects that there were two seconds to rest. Finally, subjects were asked to continue with the next trial, where the task was random.

Two comparison experiments were conducted based on two experiment paradigms (FES+VR and VR) to investigate the contribution of the FES-enhanced method to improve subjects' MI abilities. Twelve healthy subjects (age 20-27 years, mean 24±1.6 years) without a history of neurological problems participated in the experiments. All subjects are right-handed, and only two of them have MI experience. The experiments were approved by the ethics committee of Institute of Automation, Chinese Academy of Sciences. All subjects were informed of the experiment contents and signed the consent forms before the experiment. Then, these twelve subjects were randomly divided into two groups: groups A and B, and each group included six subjects. In experiment 1, the FES+VR paradigm was adopted by group A, and the VR paradigm was adopted by group B. In experiment 2, the FES+VR paradigm was adopted by group B, and the VR paradigm was adopted by group A. The scheme of the two experiments is shown in Fig. 7. To avoid the possible learning effects, the interval time between two experiments was more than thirty minutes. In each experiment, all subjects were asked to conduct thirty trials for each task. Since the signals of each trial were split into three samples by the sliding window method mentioned above, the sample number of each MI task for one subject was raised to ninety.

B. Classification Results

The classification accuracy results of experiment 1 and 2 are shown in Fig. 9. For the experiment 1, it can be seen that the relatively high classification accuracy was obtained for group A. The mean accuracy of group A is 84.48%, which is 6.31%

TABLE I
THE CLASSIFICATION PERFORMANCE COMPARISON BETWEEN FES+VR GROUP AND VR GROUP

Subejct	FES+VR group			VR group		
	ACC	F1_score	AUC	ACC	F1_score	AUC
s1	88.67±09.51	88.46±09.90	95.72±05.92	85.83±09.42	85.83±09.73	93.00±08.19
s2	79.50±10.10	79.70±10.04	85.06±11.68	64.61±16.73	61.78±21.30	69.86±18.93
s3	92.72±06.69	92.96±06.40	98.42±02.81	85.06±09.43	84.94±10.59	94.23±05.91
s4	81.94±12.94	82.40±12.50	89.70±10.80	73.06±11.93	72.43±13.69	82.58±11.89
s5	80.67±12.30	80.01±11.61	89.67±11.61	78.83±11.54	77.87±13.57	85.46±12.76
s6	83.39±09.85	82.58±12.03	92.40±07.45	80.83±10.84	80.73±11.94	89.77±09.29
s7	69.28±11.51	67.84±15.41	77.36±12.46	64.33±12.19	62.74±13.92	71.15±14.38
s8	87.39±07.23	86.78±08.87	94.93±04.55	83.61±09.59	82.89±11.43	91.52±08.92
s9	88.17±09.16	88.80±07.86	95.54±05.76	87.78±11.25	88.43±09.92	96.35±06.35
s10	95.50±05.68	95.70±05.34	99.52±01.52	78.89±09.42	78.70±09.75	88.99±09.75
s11	89.61±08.46	90.00±07.89	96.33±04.97	76.44±11.45	74.16±14.55	81.90±13.74
s12	81.11±11.69	80.10±12.65	90.38±08.85	77.94±09.29	76.58±10.90	86.41±10.62
Mean	84.83±07.03	84.61±07.48	92.09±06.23	78.10±07.63	77.26±08.46	85.93±08.46

higher than that of group B (78.17%). For the experiment 2, the mean classification accuracy of group B (85.17%) is higher 7.14% than group A (78.03%). Compared with the results of experiment 1, the classification accuracy of group A was reduced by the VR paradigm, and the classification accuracy of group B was improved by the FES+VR paradigm in experiment 2. For both groups, it can be found that the relatively high classification accuracy was achieved based on the FES+VR paradigm. Further, the paired t-test method was used to analyze the statistic difference of classification accuracies for each group between two paradigms. From the results, it can be found that there are significant improvement of classification accuracy in each group (group A: $p = 0.0263 < 0.05$; group B: $p = 0.0431 < 0.05$). However, for each experiment, the ANOVA results between two groups didn't show significance difference in statistics (experiment 1: $F = 2.66$, $p = 0.1337$; experiment 2: $F = 2.03$, $p = 0.1846$;). The reason may be that the relatively low number of subjects and the high individual variances in the MI capabilities have negative effects on the ANOVA analysis.

From the comparison results, it can be found that the classification accuracy based on FES+VR paradigm is higher than that based on VR paradigm, which was not influenced by the order of paradigms. Therefore, for further analysis, the experiment data are regrouped into the FES+VR group and VR group according to the paradigm.

The classification results of two experiments are shown in TABLE I. The best classification results and the biggest improvement are obtained by subject s10 through using the FES+VR paradigm. Significant improvement in accuracy is also found in subjects s2, s3, s4, s10, and s11. There are ten subjects with above 80% accuracy in FES+VR group, while there are only five subjects with 80% accuracy in VR group. The paired t-test results also indicate that there is a significant improvement based on FES+VR paradigm in term of ACC ($p = 0.0014 < 0.05$), F1 score ($p = 0.0021 < 0.05$), and AUC ($p = 0.0012 < 0.05$). Besides, there are three subjects (s2, s4, and s7) with below 75% classification accuracy in VR group, which may be caused by "BCI Illiteracy" problem [50]. Fortunately, using the FES+VR paradigm help these subjects obtain improvement of classification results and alleviate "BCI Illiteracy" problem.

TABLE II
THE PAIRED T-TEST RESULTS OF CHANNELS C3, CZ AND C4

Channels	p-value					
	BKM state			Idle state		
	α	β	$\alpha+\beta$	α	β	$\alpha+\beta$
C3	0.0115*	0.2295	0.0148*	0.4908	0.2828	0.2948
Cz	0.0760	0.0245*	0.0432*	0.6812	0.4249	0.6327
C4	0.0244*	0.9908	0.0537	0.9098	0.5855	0.9743

Additionally, it can be found that classification metrics are highly negatively correlated with their standard deviations. In the FES+VR group, the Pearson correlation coefficients between the metrics and the standard deviation are −0.79, −0.93, and −0.90, and those in the VR group are −0.73, −0.82, and −0.95. As shown in above results, the model with high classification performance also has better stability.

C. Analysis of Activation Intensity in the Motor Cortex

In order to analyze the activation intensity change of the motor cortex based on the different paradigms, the average PSD topographical maps for each MI state were calculated and drawn in Fig. 10. As shown in Fig. 10, the PSD of motor cortex region in the BKM state is lower than that in the idle state, which indicates that the MI indeed induced the activation of the motor cortex.

Meanwhile, by comparing the PSD in the BKM state between two groups, it can be seen that the PSD of the motor

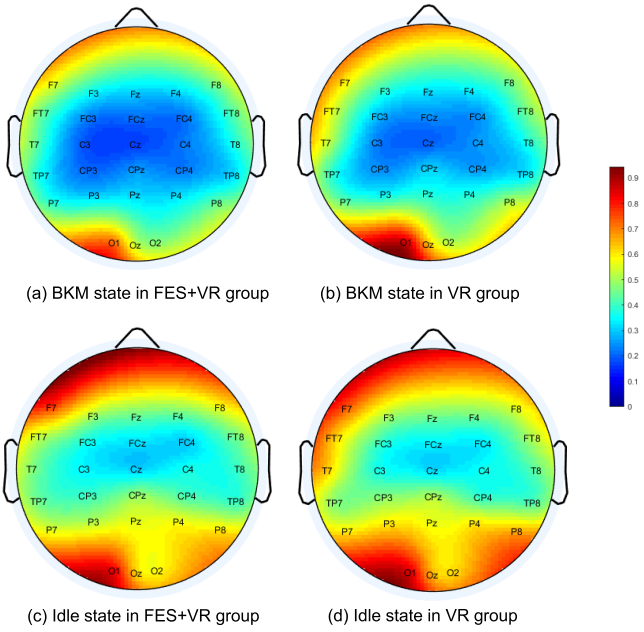

Fig. 10. The brain average PSD topographical maps for the FES+VR group and VR group during imagining BKM and idle.

cortex region in FES+VR group is lower than that in VR group. Moreover, for the idle state, there is no significant difference of PSD levels between two groups. Based on these results, it is demonstrated that the FES-enhancement only induced the differences of PSD for the BKM state between two groups. To further verify the contribution of FES-enhancement, the p value of PSD at channels C3, Cz and C4 between two groups are calculated by the paired t-test method.

The paired t-test results in α, β, $\alpha+\beta$ rhythms are shown in TABLE II. For the idle state, all p-values are far bigger than 0.05, which demonstrates there is no significant difference between the two groups. In other words, the brain activity for the idle state were not influenced by FES-enhancement. For the BKM state, there are significant difference (p=0.0115<0.05 and p=0.0244<0.05) in α rhythm at channels C3 and C4, and a significant difference (p=0.0245<0.05) in β rhythm at channel Cz can be found. For the whole 8-30Hz frequency band, i.e. $\alpha+\beta$ rhythms, there are significant differences at channels C3 and Cz. Based on the results mentioned above, it is verified that using FES+VR paradigm could help subjects perform MI task effectively and further enhance the subjects' motor cortex activation. In addition, it can be found that the frequency band with significant differences may be in α band or β band. Therefore, $\alpha+\beta$ band signals (i.e., 8-30Hz) contain the frequency band with significant differences and are more suitable for MI analysis and classification.

From the Fig. 10, it can be found that the PSD of channel C3 is lower than that of channel C4 for the BKM state. Meanwhile, as shown in TABLE II, the significant difference at channels C3 and Cz between two groups is more obvious than that at channel C4. Based on these results, it is demonstrated that the activation intensity at channels C3 and Cz (i.e., the middle and left region of motor cortex) were significantly enhanced by FES+VR paradigm.

V. Discussion

Compared with the single-mode guidance (i.e., VR), using the FES-enhanced paradigm not only help subjects obtain higher classification accuracy but also improve the classification stability. Meanwhile, based on FES+VR paradigm, the activation intensity of the motor cortex region can also be improved, particularly in channels C3 and Cz. The results of the paired t-test (p<0.05) between VR group and FES+VR group indicate that the null hypothesis should be rejected, i.e., that the statistically significant improvement of classification accuracy and activation intensity can be obtained by the FES-enhancement.

There are two possible reasons for improving the MI effects with the FES+VR paradigm. One is that the subjects' attention on the limb related to MI was improved by FES, which was consistent with the subjects' feedback. Most of the twelve subjects reported that it was not easy to lose their focus with the FES+VR paradigm. Meanwhile, it has also been demonstrated that the attention is a crucial factor in influencing the MI effects [22], [51]. Another one is that the kinesthesia illusion evoked by FES was an effective guidance for performing MI. In the study of [52], the vibrotactile stimulation was applied to the wrist toward a hybrid-modality BCI, and the high classification accuracy was obtained by imaging the motor and sensation. Compared with the mechanical vibration, the FES can induce muscles to contract and make subjects feel the deeper kinesthesia experience. When subjects performed MI tasks based on the FES+VR paradigm, the kinesthesia illusion was relatively effective guidance.

In the previous studies, it is still difficult to classify the MI patterns of the right and left lower limbs. It has been proven that movement and sensation on one side of the body are controlled by the hemisphere on the opposite side. However, the motor cortex region related to the lower limbs is relatively small and the cortexes for the right and left lower limbs are very close to each other [53]; moreover, the regions activated by imaging the left and right lower limbs are usually overlapping and located in the middle of the motor cortex; therefore, the separability between two MI patterns of the lower limbs is weak. However, from the data analysis results in Fig.10 and TABLE. II, it can be found that during imaging the right lower limb movement, the region with the high activation was located in the middle and left of the motor cortex, i.e., at channels C3 and Cz. In particular, the activation intensity at channels C3 and Cz in FES+VR group was higher than that in VR group. It is indicated that the spatial resolution of MI patterns for the lower limbs may be improved by using the FES+VR paradigm. We hypothesize that if subjects imagine the left lower limb, the high activation region may be located in the middle and right region of the motor cortex, which is beneficial to distinguish the MI patterns of the right and left lower limbs. In future work, this hypothesis is to be verified by the experiment.

Additionally, it is worth noting that the PSD for the BKM state is lower than that for idle state in the frontal lobe region. The PSD in the frontal lobe region is related to the subjects' attention state [54]. In our previous work [55], an attention

classifier was built by calculating the PSD in the frontal lobe region. Therefore, the attention mechanism can be integrated into the MI-BCI to build a hybrid-modality BCI.

Although the effectiveness of the proposed FES+VR paradigm has been validated on twelve subjects, more subjects, including patients, are need to be involved in the experiments for further analysis in the future. Meanwhile, in order to make the muscle contraction feeling produced by FES more similar to that in the actual movement, the current change of FES should be further optimized, and more associated muscles can also be given FES.

VI. Conclusion

In this study, an enhanced MI-BCI based on FES and VR was proposed to help subjects perform MI effectively. The performance of proposed MI-BCI was validated through the comparison experiments on twelve subjects. The experiment results showed that the classification performance was significantly improved ($p<0.05$) by using the FES+VR paradigm; meanwhile, the activation intensity of the motor cortex based on the FES+VR paradigm was higher than that based on the VR paradigm, especially at channels C3 and Cz. Furthermore, the proposed MI-BCI will be combined with the rehabilitation robot to provide effective rehabilitation strategies in our future work.

Acknowledgment

The authors would like to thank all volunteers for their participation in the experiments.

References

[1] A. Frisoli, M. Solazzi, C. Loconsole, and M. Barsotti, "New generation emerging technologies for neurorehabilitation and motor assistance," *Acta Myologica*, vol. 35, no. 3, pp. 141–144, 2016.

[2] M. A. Schwemmer *et al.*, "Meeting brain-computer interface user performance expectations using a deep neural network decoding framework," *Nature Med.*, vol. 24, no. 11, pp. 1669–1676, Nov. 2018.

[3] R. Foong *et al.*, "Assessment of the efficacy of EEG-based MI-BCI with visual feedback and EEG correlates of mental fatigue for upper-limb stroke rehabilitation," *IEEE Trans. Biomed. Eng.*, vol. 67, no. 3, pp. 786–795, Mar. 2020.

[4] A. Solodkin, P. Hlustik, E. E. Chen, and S. L. Small, "Fine modulation in network activation during motor execution and motor imagery," *Cerebral Cortex*, vol. 14, no. 11, pp. 1246–1255, Nov. 2004.

[5] M. Barsotti, D. Leonardis, N. Vanello, M. Bergamasco, and A. Frisoli, "Effects of continuous kinaesthetic feedback based on tendon vibration on motor imagery BCI performance," *IEEE Trans. Neural Syst. Rehabil. Eng.*, vol. 26, no. 1, pp. 105–114, Jan. 2018.

[6] G. Nelles, W. Jentzen, M. Jueptner, S. Müller, and H. C. Diener, "Arm training induced brain plasticity in stroke studied with serial positron emission tomography," *NeuroImage*, vol. 13, no. 6, pp. 1146–1154, Jun. 2001.

[7] A. R. C. Donati *et al.*, "Long-term training with a brain-machine interface-based gait protocol induces partial neurological recovery in paraplegic patients," *Sci. Rep.*, vol. 6, no. 1, p. 30383, Sep. 2016.

[8] R. Gentili, C. E. Han, N. Schweighofer, and C. Papaxanthis, "Motor learning without doing: Trial-by-trial improvement in motor performance during mental training," *J. Neurophysiology*, vol. 104, no. 2, pp. 774–783, Aug. 2010.

[9] V. K. Ranganathan, V. Siemionow, J. Z. Liu, V. Sahgal, and G. H. Yue, "From mental power to muscle power-gaining strength by using the mind," *Neuropsychologia*, vol. 42, no. 7, pp. 944–956, Jan. 2004.

[10] R. J. Gentili and C. Papaxanthis, "Laterality effects in motor learning by mental practice in right-handers," *Neuroscience*, vol. 297, pp. 231–242, Jun. 2015.

[11] Y. Zhang *et al.*, "Multi-kernel extreme learning machine for EEG classification in brain-computer interfaces," *Expert Syst. Appl.*, vol. 96, pp. 302–310, Apr. 2018.

[12] J. Li, Z. Struzik, L. Zhang, and A. Cichocki, "Feature learning from incomplete EEG with denoising autoencoder," *Neurocomputing*, vol. 165, pp. 23–31, Oct. 2015.

[13] F. Qi, Y. Li, and W. Wu, "RSTFC: A novel algorithm for spatio-temporal filtering and classification of single-trial EEG," *IEEE Trans. Neural Netw. Learn. Syst.*, vol. 26, no. 12, pp. 3070–3082, Dec. 2015.

[14] X. Xie, Z. L. Yu, Z. Gu, J. Zhang, L. Cen, and Y. Li, "Bilinear regularized locality preserving learning on Riemannian graph for motor imagery BCI," *IEEE Trans. Neural Syst. Rehabil. Eng.*, vol. 26, no. 3, pp. 698–708, Mar. 2018.

[15] L. He, Y. Hu, Y. Li, and D. Li, "Channel selection by Rayleigh coefficient maximization based genetic algorithm for classifying single-trial motor imagery EEG," *Neurocomputing*, vol. 121, pp. 423–433, Dec. 2013.

[16] M. Arvaneh, C. Guan, K. K. Ang, and C. Quek, "Optimizing the channel selection and classification accuracy in EEG-based BCI," *IEEE Trans. Biomed. Eng.*, vol. 58, no. 6, pp. 1865–1873, Jun. 2011.

[17] N. Lu, T. Li, X. Ren, and H. Miao, "A deep learning scheme for motor imagery classification based on restricted Boltzmann machines," *IEEE Trans. Neural Syst. Rehabil. Eng.*, vol. 25, no. 6, pp. 566–576, Jun. 2017.

[18] Y. R. Tabar and U. Halici, "A novel deep learning approach for classification of EEG motor imagery signals," *J. Neural Eng.*, vol. 14, no. 1, Feb. 2017, Art. no. 016003.

[19] O.-Y. Kwon, M.-H. Lee, C. Guan, and S.-W. Lee, "Subject-independent brain-computer interfaces based on deep convolutional neural networks," *IEEE Trans. Neural Netw. Learn. Syst.*, early access, Nov. 13, 2019, doi: 10.1109/TNNLS.2019.2946869.

[20] B. Xia, Q. Zhang, H. Xie, and J. Li, "A neurofeedback training paradigm for motor imagery based brain-computer interface," in *Proc. Int. Joint Conf. Neural Netw. (IJCNN)*, Jun. 2012, pp. 1–4.

[21] X. Xie, Z. L. Yu, H. Lu, Z. Gu, and Y. Li, "Motor imagery classification based on bilinear sub-manifold learning of symmetric positive-definite matrices," *IEEE Trans. Neural Syst. Rehabil. Eng.*, vol. 25, no. 6, pp. 504–516, Jun. 2017.

[22] Z. Qiu *et al.*, "Optimized motor imagery paradigm based on imagining Chinese characters writing movement," *IEEE Trans. Neural Syst. Rehabil. Eng.*, vol. 25, no. 7, pp. 1009–1017, Jul. 2017.

[23] G. Pfurtscheller *et al.*, "Viewing moving objects in virtual reality can change the dynamics of sensorimotor EEG rhythms," *Presence, Teleoperators Virtual Environ.*, vol. 16, no. 1, pp. 111–118, Feb. 2007.

[24] T. Sollfrank, D. Hart, R. Goodsell, J. Foster, and T. Tan, "3D visualization of movements can amplify motor cortex activation during subsequent motor imagery," *Frontiers Hum. Neurosci.*, vol. 9, p. 463, Aug. 2015.

[25] Y. Bian, H. Qi, L. Zhao, D. Ming, T. Guo, and X. Fu, "Improvements in event-related desynchronization and classification performance of motor imagery using instructive dynamic guidance and complex tasks," *Comput. Biol. Med.*, vol. 96, pp. 266–273, May 2018.

[26] S. Liang, K.-S. Choi, J. Qin, W.-M. Pang, Q. Wang, and P.-A. Heng, "Improving the discrimination of hand motor imagery via virtual reality based visual guidance," *Comput. Methods Programs Biomed.*, vol. 132, pp. 63–74, Aug. 2016.

[27] D. Zapała *et al.*, "The impact of different visual feedbacks in user training on motor imagery control in BCI," *Appl. Psychophysiology Biofeedback*, vol. 43, no. 1, pp. 23–35, Mar. 2018.

[28] S. Bhattacharyya, M. Clerc, and M. Hayashibe, "Augmenting motor imagery learning for brain-computer interfacing using electrical stimulation as feedback," *IEEE Trans. Med. Robot. Bionics*, vol. 1, no. 4, pp. 247–255, Nov. 2019.

[29] J. Cantillo-Negrete, R. I. Carino-Escobar, P. Carrillo-Mora, J. A. Barraza-Madrigal, and O. Arias-Carrión, "Robotic orthosis compared to virtual hand for brain-computer interface feedback," *Biocybernetics Biomed. Eng.*, vol. 39, no. 2, pp. 263–272, Apr. 2019.

[30] D. J. McFarland, L. M. McCane, and J. R. Wolpaw, "EEG-based communication and control: Short-term role of feedback," *IEEE Trans. Rehabil. Eng.*, vol. 6, no. 1, pp. 7–11, Mar. 1998.

[31] C. Zuo *et al.*, "Novel hybrid brain-computer interface system based on motor imagery and P300," *Cognit. Neurodynamics*, vol. 14, pp. 253–265, Oct. 2019.

[32] C. E. King, P. T. Wang, L. A. Chui, A. H. Do, and Z. Nenadic, "Operation of a brain-computer interface walking simulator for individuals with spinal cord injury," *J. Neuroeng. Rehabil.*, vol. 10, no. 1, p. 77, 2012.

[33] Z. Yu, L. Li, J. Song, and H. Lv, "The study of visual-auditory interactions on lower limb motor imagery," *Frontiers Neurosci.*, vol. 12, p. 509, Jul. 2018.
[34] D. J. McFarland, L. M. McCane, S. V. David, and J. R. Wolpaw, "Spatial filter selection for EEG-based communication," *Electroencephalogr. Clin. Neurophysiol.*, vol. 103, no. 3, pp. 386–394, Sep. 1997.
[35] K. J. Miller, G. Schalk, E. E. Fetz, M. den Nijs, J. G. Ojemann, and R. P. N. Rao, "Cortical activity during motor execution, motor imagery, and imagery-based online feedback," *Proc. Nat. Acad. Sci. USA*, vol. 107, no. 9, pp. 4430–4435, Mar. 2010.
[36] Y. Liu, H. Zhang, M. Chen, and L. Zhang, "A boosting-based spatial-spectral model for stroke patients' EEG analysis in rehabilitation training," *IEEE Trans. Neural Syst. Rehabil. Eng.*, vol. 24, no. 1, pp. 169–179, Jan. 2016.
[37] Y. Zhang, G. Zhou, J. Jin, X. Wang, and A. Cichocki, "Optimizing spatial patterns with sparse filter bands for motor-imagery based brain-computer interface," *J. Neurosci. Methods*, vol. 255, pp. 85–91, Nov. 2015.
[38] K. T. Ragnarsson, "Functional electrical stimulation after spinal cord injury: Current use, therapeutic effects and future directions," *Spinal Cord*, vol. 46, no. 4, pp. 255–274, 2008.
[39] O. A. Howlett, N. A. Lannin, L. Ada, and C. McKinstry, "Functional electrical stimulation improves activity after stroke: A systematic review with meta-analysis," *Arch. Phys. Med. Rehabil.*, vol. 96, no. 5, pp. 934–943, May 2015.
[40] S. Qiu *et al.*, "Event-related beta EEG changes during active, passive movement and functional electrical stimulation of the lower limb," *IEEE Trans. Neural Syst. Rehabil. Eng.*, vol. 24, no. 2, pp. 283–290, Feb. 2016.
[41] J. Müller-Gerking, G. Pfurtscheller, and H. Flyvbjerg, "Designing optimal spatial filters for single-trial EEG classification in a movement task," *Clin. Neurophysiol.*, vol. 110, no. 5, pp. 787–798, May 1999.
[42] B. Blankertz, R. Tomioka, S. Lemm, M. Kawanabe, and K.-R. Müller, "Optimizing spatial filters for robust EEG single-trial analysis," *IEEE Signal Process. Mag.*, vol. 25, no. 1, pp. 41–56, Dec. 2007.
[43] A. M. Elnady *et al.*, "A single-session preliminary evaluation of an affordable BCI-controlled arm exoskeleton and motor-proprioception platform," *Frontiers Hum. Neurosci.*, vol. 9, p. 168, Mar. 2015.
[44] K. Keng Ang, Z. Yang Chin, H. Zhang, and C. Guan, "Filter bank common spatial pattern (FBCSP) in brain-computer interface," in *Proc. IEEE Int. Joint Conf. Neural Netw. (IEEE World Congr. Comput. Intell.)*, Hong Kong, Jun. 2008, pp. 2390–2397.
[45] S.-H. Park, D. Lee, and S.-G. Lee, "Filter bank regularized common spatial pattern ensemble for small sample motor imagery classification," *IEEE Trans. Neural Syst. Rehabil. Eng.*, vol. 26, no. 2, pp. 498–505, Feb. 2018.
[46] F. Lotte and C. Guan, "Regularizing common spatial patterns to improve BCI designs: Unified theory and new algorithms," *IEEE Trans. Biomed. Eng.*, vol. 58, no. 2, pp. 355–362, Feb. 2011.
[47] Y. Xiaofang and W. Yaonan, "Parameter selection of support vector machine for function approximation based on chaos optimization," *J. Syst. Eng. Electron.*, vol. 19, no. 1, pp. 191–197, Feb. 2008.
[48] C.-C. Chang and C.-J. Lin, "LIBSVM: A library for support vector machines," *ACM Trans. Intell. Syst. Technol.*, vol. 2, no. 3, pp. 1–27, Apr. 2011.
[49] M. Lotze and U. Halsband, "Motor imagery," *J. Physiol.-Paris*, vol. 99, nos. 4–6, pp. 386–395, 2006.
[50] A. Nijholt and D. Tan, "Brain-computer interfacing for intelligent systems," *IEEE Intell. Syst.*, vol. 23, no. 3, pp. 72–79, May 2008.
[51] I. Nojima, S. Koganemaru, T. Kawamata, H. Fukuyama, and T. Mima, "Action observation with kinesthetic illusion can produce human motor plasticity," *Eur. J. Neurosci.*, vol. 41, no. 12, pp. 1614–1623, Jun. 2015.
[52] L. Yao, J. Meng, D. Zhang, X. Sheng, and X. Zhu, "Combining motor imagery with selective sensation toward a hybrid-modality BCI," *IEEE Trans. Biomed. Eng.*, vol. 61, no. 8, pp. 2304–2312, Aug. 2014.
[53] P. Boord, A. Craig, Y. Tran, and H. Nguyen, "Discrimination of left and right leg motor imagery for brain-computer interfaces," *Med. Biol. Eng. Comput.*, vol. 48, no. 4, pp. 343–350, Apr. 2010.
[54] R. A. Barkley, G. Grodzinsky, and G. J. DuPaul, "Frontal lobe functions in attention deficit disorder with and without hyperactivity: A review and research report," *J. Abnormal Child Psychol.*, vol. 20, no. 2, pp. 163–188, Apr. 1992.
[55] J. Wang *et al.*, "BCI and multimodal feedback based attention regulation for lower limb rehabilitation," in *Proc. Int. Joint Conf. Neural Netw. (IJCNN)*, Budapest, Hungary, Jul. 2019, pp. 1–7.